Network-based analysis reveals microRNA regulation of oncogenic pathways in SOX10-depleted uveal melanoma

Chunyan Luan[1], Anja Wessely[1], Zhesi Zhang[2], Liang Zhang[2], Adrian Weich[1,3,4], Christopher Lischer[1], Carola Berking[1,3,4], Markus V. Heppt[1], Julio Vera[1,3,4,#], Xin Lai[1,2,5,#]

[1]Department of Dermatology, Universitätsklinikum Erlangen, CCC Erlangen-EMN, Friedrich-Alexander-Universität Erlangen-Nürnberg, 91054 Erlangen, Germany

[2]Biomedicine Unit, Faculty of Medicine and Health Technology, Tampere University, Tampere, Finland

[3]Deutsches Zentrum Immuntherapie, Erlangen, Germany

[4]Comprehensive Cancer Center Erlangen, Erlangen, Germany

[5]TAYS Cancer Centre, Tampere University Hospital, Wellbeing Services County of Pirkanmaa, Tampere, Finland

[#]Corresponding author:

Julio Vera (julio.vera-gonzalez@uk-erlangen.de; +4991318545876), Uniklinikum Erlangen, Erlangen, Germany; Xin Lai (xin.lai@tuni.fi; +358505751673), Faculty of Medicine and Health Technology, Tampere University, Tampere, Finland.

Abstract

SOX10 is essential for melanocyte development and maintenance and plays a critical role in uveal melanoma (UM) initiation and progression. While SOX10's transcriptional regulation of protein-coding genes is well characterized, its role on microRNA (miRNA) regulatory landscape in UM remains unexplored. Here, we employed network-based modeling to systematically characterize miRNA regulatory functions following SOX10 depletion in UM. First, we profiled mRNA and miRNA expression levels in SOX10 wild-type and knockdown UM cells. Then, we integrated the transcriptomic data, a UM network, and a Bayesian model to quantify miRNAs' regulatory activities and identify key miRNAs. Subsequently, we employed pathway enrichment analysis combined with literature mining to elucidate the functional roles of identified miRNAs through their target genes and associated signaling pathways in UM. We identified 17 miRNAs that show significant changes in regulatory activities following SOX10 knockdown in UM cells. These miRNAs regulate the expression of genes involved in cancer hallmark pathways, including cell cycle progression, mTORC1 signaling, and fatty acid metabolism. Notably, miR-34a, miR-25, miR-186, and miR-211 have tumor-suppressive potential by targeting genes involved in UM progression and metastasis. Our results suggested that SOX10 depletion in UM can activate tumor-suppressive mechanisms through regulating miRNAs.

Keywords: SOX10, microRNA, uveal melanoma, systems biology, network biology,

INTRODUCTION

Uveal melanoma (UM), the most common intraocular tumor in adults, arises from melanocytes in the choroid, ciliary body, or iris (1), but is far rarer than cutaneous melanoma (CM) and classified as an orphan cancer (2). Despite both tumors originating from melanocytes, UM and CM differ in tumor biology, clinical characteristics, and treatment options (3). An example of these differences is SOX10, a member of the SOX family of transcription factors that plays a critical role in neural crest development and the differentiation of various neural crest derivatives, including the melanocyte lineage (4–6). While SOX10 has been extensively studied in CM and is recognized for its crucial role in promoting tumor progression in melanoma (7–9), the knowledge about its function in UM remains limited, with a few studies showing that SOX10 has similar functions across UM lineages, such as strong nuclear expression regardless of their origins (10). SOX10 is expressed diffusely across 11 UM cell lines and in surrounding uveal or choroidal melanocytes (11). While SOX10 expression is typically consistent, a pathogenic SOX10 mutation is identified in a single UM patient, suggesting the existence of rare genetic subtypes with distinct biological characteristics (12). Mechanistically, SOX10 ablation, downregulating the expression of GAPDH, significantly suppresses UM growth and proliferation *in vivo* (13). BAF inhibition leads to the loss of enhancer occupancy by SOX10 and its interacting partner MITF, resulting in down-regulation of the melanocytic gene expression program in UM (14). In clinical applications, SOX10 serves as a critical diagnostic marker, exhibiting exclusive nuclear positivity in all 38 cases of a UM cohort and representing a sensitive marker for UM diagnosis (10).

SOX10 is a critical regulator in tumor progression, with its multifaceted functions involved in cell apoptosis, proliferation, and migration (15). Its regulatory landscape is further intricated by other molecules, such as microRNAs (miRNAs), which are a class of non-coding RNAs with 22-25 nucleotides in length. By modulating the transcription and translation of specific protein-coding and non-coding genes such as circular RNAs, miRNAs can alter cellular behavior and influence the outcomes of various cellular processes alone or in a combined manner (16–21). Growing evidence suggests that miRNAs play a crucial role in the development and progression of UM (22–24). They act as vital regulators of complex signaling networks by targeting key genes involved in tumor growth, invasion, and metastasis (23, 25, 26). For example, the miR-181 family acts as a negative regulator of CTDSPL-mediated cell cycle progression (27). The long non-coding RNA ZNF197-AS1 also inhibits uveal melanoma cell proliferation, migration, and invasion by sponging miR-425, which upregulates GABARAPL1 (28). Additionally, miR-34a suppresses the migration and invasion of these cells through its negative control of LGR4 (29). Furthermore, miRNAs hold significant potential as diagnostic biomarkers (30–33) and therapeutic agents, either as monotherapy or in combination treatments, to target and modulate gene expression in cancer such as UM (34–36). miRNA-

77 mediated regulatory circuits are crucial for tumor plasticity by controlling, for example the
78 dynamics of SOX10 expression levels (37). Though SOX10-deficient CM cells have been
79 reported to be associated with therapeutic resistance (38) and invasive phenotypes (39), there
80 has been no investigation into altered miRNA profiles in UM, which prevents our understanding
81 of the SOX10-mediated miRNA landscape in this malignancy. To address this knowledge gap,
82 we investigated SOX10-mediated miRNA regulation and their regulatory profiles in UM. We
83 hypothesized that SOX10 modulates specific miRNAs to coordinate downstream pathways
84 involved in UM progression. Identifying key miRNAs that regulate tumor growth and
85 proliferation may therefore provide deeper insights into SOX10's mechanistic role in UM
86 pathogenesis.

87 Here, we present a network-based approach to identify miRNAs regulated by SOX10 in UM
88 (Figure 1). With this approach, we aim to characterize SOX10-mediated miRNA expression
89 and regulatory profiles for better an understanding of the molecular function of miRNAs in UM.
90 Specifically, we performed high-throughput RNA sequencing to obtain genome-wide
91 transcriptomic profiles (including protein-coding genes and miRNAs) in SOX10-knockdown
92 (SOX10-KD) UM cells. Next, we integrated the gene expression data with a UM network to
93 quantify the regulatory activity of miRNAs. Then, we identified driver miRNAs that show
94 significant changes in the regulatory activity of SOX10-KD UM cells, and we elaborated the
95 molecular mechanisms through which these miRNAs can influence tumor phenotypes at the
96 pathway level. Taken together, we demonstrated the power of network medicine approaches
97 to identify functional miRNA-gene interactions with therapeutic potential in UM.

98 **MATERIALS AND METHODS**

99 **Experimental design and cell culture**

100 We used two UM cell lines (92.1 and Mel270) to investigate gene expression profiles (including
101 mRNA and miRNA) under two experimental conditions: SOX10 knockdown (SOX10-KD) and
102 control. The experimental design included four biological replicates for each cell line under
103 each condition, resulting in a total of 16 samples.

104 UM cell lines 92.1 (RRID:CVCL_8607) and Mel270 (RRID:CVCL_C302) were kindly provided
105 by Klaus Griewank, University Hospital Essen, Germany. The cells were cultured in RPMI1640
106 medium containing 2 mM L-glutamine (Gibco by Life Technologies, Waltham, Massachusetts,
107 USA), 10% fetal bovine serum (FBS; Merck, Darmstadt, Germany), and 1x antibiotic-
108 antimycotic (Invitrogen, Waltham, Massachusetts, USA) in a humidified incubator at 37°C and
109 5% CO2 atmosphere. The cells were regularly tested for mycoplasma contamination using the
110 Venor®GeM Classic Mycoplasma Detection Kit for conventional PCR (Minerva Biolabs, Berlin,
111 Germany) according to the manufacturer's instructions.

112

113 **siRNA transfection**

114 For SOX10-KD, cells were seeded in 6-well plates in RPMI1640 medium containing 2 mM L-
115 glutamine and 10% FBS without 1× antibiotic-antimycotic supplement and transfected the
116 following day with 20 nM siRNAs: siSOX10-B (sequence 5'-GUAUGCAGCACAAGAAAGATT-
117 3') (40) or control siRNA with a random sequence that does not match the human genome
118 (sequence 5'-GCGCAUUCCAGCUUACGUA-3' with asymmetric dTdT overhang at the 3' end;
119 both from Eurofins Genomics, Ebersberg, Germany) using 1.25 µl Lipofectamine RNAiMAX
120 (Invitrogen) per well. All cells were cultivated at 37°C and 5% CO2 atmosphere in a humidified
121 incubator for 24 h.

122

123 **Total RNA extraction and qPCR to test efficacy of SOX10 knockdown**

124 Total RNA was extracted 24 h after transfection using the miRNeasy Tissue Cells Advanced
125 Kit including a DNase digestion step to eliminate genomic DNA contamination using the
126 RNase-Free DNase Set (Qiagen, Hilden, Germany). RNA concentration was determined with
127 a Nanodrop 2000 spectrophotometer (Thermo). SOX10-KD efficacy was assessed by
128 quantitative real-time PCR (qPCR) before sequencing. Therefore, 1000 ng of total RNA were
129 transcribed to cDNA using the Expand™ Reverse Transcriptase Kit (Roche, Penzberg,
130 Germany) and oligo(dT)- oligonucleotide primers (Eurofins Genomics, Ebersberg, Germany).
131 The LightCycler® TaqMan® Master Kit (Roche), 200 nM of forward and reverse primers

designed with the software “Assay Design Center” (Roche) (Table S1), 100 nM primer-matched hydrolysis probes from the Universal ProbeLibrary set human (Roche), and 50 ng cDNA were used to carry out the qPCR on a qTower3 instrument (Analytik Jena, Jena, Germany). Gene expression was normalized to glyceraldehyde 3-phosphate dehydrogenase expression (GAPDH).

RNA sequencing data processing and analysis

RNA sequencing analysis of pooled total RNA derived from four individual experiments was performed by CeGaT (Tübingen, Germany) using the KAPA RNA HyperPrep Kit with RiboErase (Roche) for library preparation and a NovaSeq™ 6000 instrument (Illumina, San Diego, California, USA) for sequencing. RNA quality was checked on a Bioanalyzer 2100 (Agilent Technologies, Santa Clara, California, USA) before RNA sequencing.

Quality control and quantification of mRNA and miRNA sequencing data. In our previous work, we used a standard bioinformatics pipeline to process mRNA sequencing data (41). Specifically, the raw sequencing data in FastQ format underwent quality control with FastQC (version 0.11.9) and trimming to remove adapters using TrimGalore (version 0.6.6). Then, the obtained reads were mapped to the human reference genome assembly GRCh38 (hg38) with Gencode Annotation (version 22) (42) by STAR (version 2.0201) (43). Finally, transcript quantification was made using StringTie (version 2.1.4), which accurately estimates the read counts for each transcript.

We used MultiQC to check the quality of the miRNA sequencing data (44) (Table S2). The sequencing data underwent comprehensive quality checks, including evaluation of base quality via Phred scores, assessment of sequence duplication levels to detect potential contamination or amplification bias, and analysis of sequence integrity after adapter removal. Additional quality control measures included examination of GC content and distribution of unspecific bases (or N bases) to identify possible sequencing biases. Then, we trimmed the reads by removing adapters using Trimmomatic (version 0.39) and retained good reads using fastq_quality filter with the parameters (-Q33 -q 20 -p 80). The trimmed reads were mapped to the human genome hg38 using STAR (version 2.7.3a) using the default parameters. After the alignment, we used samtools to convert and sort the sequence alignment/map files. Finally, miRNA read counts were quantified using FeatureCounts (version 2.0.1) using the human genome hg38.

Gene expression analysis. For gene expression analysis, Ensembl IDs were converted to gene symbols using the GRCh38 and miRNAs were named using mature miRNA names from miRbase (45). After the conversion, duplicate gene symbols were resolved by adding their

167 expression values. We eliminated the batch effects of both mRNA and miRNA samples using
168 *ComBat* in the R package *sva* (46). It is an empirical Bayesian method that can effectively
169 adjust batch effects while retaining biological variation in the data. We performed principal
170 component analysis (PCA) to visualize the results (Figure S2).

171

172 **Network modeling and analysis using NetBID2**

173 We used NetBID2 to perform network modelling and analysis. It is a method that uses a
174 network-based Bayesian inference method to identify drivers and shows its power to identify
175 crucial genes with mild changes in their expression profiles (47, 48). The method is to identify
176 drivers in gene regulatory networks, such as transcription factors (TF), signaling proteins, and
177 miRNAs. In our case, the identified miRNAs are regarded as important regulators in a SOX10-
178 mediated UM network. We merged the miRNA and mRNA expression profiles (Table S3) and
179 obtained an overview of the data (Figure S3). Next, we normalized the data and performed a
180 log2 transformation. The normalization method adds one to each gene's raw count and
181 multiplies it by a scaling factor, which is the mean sequence depth of all samples divided by
182 the sum of the sequence depth of the corresponding sample. Finally, we filtered out genes
183 whose expression values are at or below the fifth percentile in 90% or more of the samples,
184 indicating that they are essentially not expressed in most samples.

185 ***The UM network reconstruction***. We reconstructed a SOX10-centered gene regulatory
186 network using annotated information containing the most relevant intracellular signaling
187 pathways in UM through literature survey. The network was developed based on SOX10
188 interacting protein and further expanded and pruned using databases and available gene
189 expression data for UM (see SM for details)(41). As a result, we obtained a SOX10-centered
190 UM network with 2,149 nodes (including 28 miRNAs) and 7,832 edges (SM Excel S1). As the
191 16 UM samples' mRNA and miRNA profiles are not paired, we divided them into four groups
192 using matching cell lines (i.e. 92.1 and MEL270) and experimental conditions (control and
193 SOX10-KD) (Table S3). We used the average expression levels of the four groups to compute
194 Spearman correlation coefficients for interacting genes. Since the primary function of miRNAs
195 is to repress gene expression in mammals (49), in our network we considered miRNA-mRNA
196 interactions with negative correlation values as relevant and removed the interactions with
197 positive values. The resulting regulatory network data, together with gene expression profiles,
198 were used as inputs for performing differential gene expression (DE) and differential activity
199 (DA) analysis.

200 ***Differential Expression and Activity inference.*** We used NetBID2, which uses a Bayesian
201 linear modelling approach, for performing DA and DE analysis between SOX10-KD and control
202 samples (48). Differentially expressed genes with an adjusted p-value ≤ 0.05 and |log2FC| ≥ 1

are considered significant. In our analysis, a gene's activity is high when its up or downregulation manifests in the over or underexpression of its target genes. We used this method to infer miRNAs' activity based on the correlation between the expression profiles of miRNAs and their targets. This analysis allowed us to quantify the functional impact of a miRNA within the regulatory network by measuring its downstream repressive effects rather than relying solely on its own expression level. The resulting activity score can be considered a metric of the miRNA's regulatory influence within SOX10-KD UM cells. Mathematically, the activity score of a driver gene is computed using the following equation:

$$AS_{<source_i, sample_n>} = \frac{MI_{<source_i, target_j>} \times Exp_{<target_j,\ sample_n>}}{num\ of\ target_{source_i}},$$

Where $MI_{<i,j>}$ is a matrix representing mutual information between source gene *i* (such as miRNAs), and target gene *j* (such as miRNA targets). $Exp_{<j,n>}$ is a matrix representing the expression of target *j* in sample *n*. The multiplication of the two matrices results in a score for source gene *i* in sample *n*, which is calculated by summing the expression levels of all targets in sample *n*, weighted by their mutual information with the specific source *i.* The source gene's activity score is normalized by the number of the source gene's targets. The sample-based genes' activity scores ($AS_{<i,n>}$) are used to conduct DA analysis between SOX10-KD and control samples using a Bayesian linear model. Genes with an adjusted p-value ≤ 0.05 are considered to have significant change in DA. The full results for DE and DA analysis can be found in SM Excel S2 and S3, respectively.

Gene set enrichment analysis

We used Enrichr (50) to conduct gene set enrichment analysis for the 50 hallmark gene sets from MSigDB (51). The hallmark collection represents a refined, curated subset of gene sets designed to summarize well-defined biological states or processes with coherent expression patterns. For the background gene list, we used all genes in the UM network. For the input gene list, we used target genes of miRNAs with significant change in DA (adj. p-value ≤ 0.05). Gene sets with an adjusted p-value ≤ 0.05 were considered significant. In addition, the results included the pathways' odds ratio and combined score (i.e., -log10(adj. p-value) multiplied by Z-score), where Z-score is a measure of the "deviation from the expected range" or the "deviation from the expected number of overlapping genes". This combined score is related to the degree of enrichment, considering the size of the gene set and the total number of genes. The full results can be found in SM Excel S4.

Results

Integration of miRNA and mRNA data

We performed comprehensive quality control to check the reliability of miRNA sequencing data measured in UM cell lines. Although the data show good quality reflected by Phred Scores, we observed some abnormal and unusual incidences known to be common for miRNA sequencing data (Table S2). Specifically, the data has a high GC content, which skews the overall GC distribution. Due to the short size of miRNAs, the data shows a narrow sequence length distribution. In addition, certain miRNAs are usually highly abundant in cells (e.g., let-7 family miRNAs), leading to a higher proportion of miRNA overrepresented sequences compared to mRNAs (52). The overall diversity of miRNAs is generally lower than that of total RNA, leading to an increased proportion of duplicated sequences. However, the comprehensive quality check suggests that our miRNA data is of good quality and in line with data from other melanoma cell lines (53, 54).

We also generated comprehensive RNA sequencing data from matched SOX10-KD experiments in the same UM cell lines (i.e. 92.1 and Mel270) (41). Thus, we merged these complementary miRNA and transcriptomic datasets to investigate the regulatory network affected by SOX10-KD in UM cells, with particular emphasis on identifying miRNA-mediated mechanisms of gene regulation (Figure 1).

Following the data integration, we conducted quality control analyses to identify potential confounding factors. We used principal component analysis (PCA) to assess data heterogeneity and detected pronounced sample clustering based on cell line origin in the integrated gene expression profiles, indicating substantial batch effects that could obscure biological signals of interest (Figure S2). To preserve the SOX10-KD effect while minimizing technical variation, we applied a linear mixed-effects model to remove cell line-associated batch effects while retaining biologically relevant variation. Subsequent PCA validation confirmed the elimination of cell line-dependent clustering patterns while maintaining experimental group separation based on SOX10 status (Figure S3A), ensuring that subsequent comparison analysis reflects actual biological differences.

Furthermore, we found that the combined mRNA and miRNA expression profiles can distinguish SOX10-KD from control samples, with 6 out of 8 SOX10-KD samples clustering together and the remaining two clustering with control samples based on their expression profile distances (Figure S3B). All samples had many genes expressed at low levels (Figure S3C) and exhibited high correlation (Figure S3D). SOX10-KD resulted in massive change of gene expression, consistent with SOX10's role as an important TF that regulates numerous genes in the melanocytic lineage and whose deregulation can substantially alter the transcriptomic landscape, as demonstrated in melanoma (39).

273 **SOX10 knockdown leads to massive transcriptomic change in UM**

274 To characterize the effects of SOX10-KD in UM cells, we performed differential gene (DE)
275 expression analysis. We identified 2,222 up-regulated and 1,156 down-regulated protein-
276 coding genes with at least 2-fold changes (Figure 2A and SM Excel S2). The most significantly
277 up-regulated genes (based on adjusted p-value) are BMF, FOXO1, and HSPB7, while the most
278 down-regulated genes are KPNB1, GNPDA1, and RIOX2. The upregulated genes are reported
279 to be related to tumorigenesis and development of UM. Specifically, BMF acts as a key
280 mediator of apoptosis in UM, and it is targeted by miRNAs like miR-221 and miR-125b in
281 cancer (55, 56). Its downregulation, particularly in response to HGF/cMET signaling, is a major
282 mechanism by which UM cells acquire resistance to MEK inhibitors (57). An *in vitro* study
283 indicated that HGF promotes resistance to MEK inhibitors by increasing the protein
284 expressions of BCL2L11 and BMF in UM (58). Somatic mutations in FOXO1 are associated
285 with increased metastatic potential and poorer prognosis in UM patients (59), and the gene is
286 known to regulate multiple miRNAs in the context of cancer (60) . HSPB7 is found to be
287 expressed in UM subclusters in single-cell RNA-seq experiments (61) but there is no direct
288 experimental evidence detailing its mechanistic role in UM. In contrast, the downregulated
289 genes involvement in UM pathogenesis and progression remains to be investigated, but they
290 are known to play a role in other cancers, for example KPNB1 in melanoma (62), GNPDA1 in
291 several cancers (63) and RIOX2 in lung and prostate cancers (64, 65).

292 In addition, we identified six DE miRNAs including miR-664b-5p, miR-4498, miR-6772-3p that
293 are significantly upregulated while miR-5002-5p, miR-6509-3p, and miR-190b-5p are
294 significantly downregulated (Figure 2A). Though some of these miRNAs are involved in tumor
295 progression, such as loss of miR-664b enhances malignancy of cutaneous melanoma (66) and
296 miR-190b is a tumor suppressor in lung cancer (67), there is no evidence describing their
297 association with UM.

298 Taken together, SOX10-KD in UM can massively alter transcriptomic landscape including
299 mRNAs and miRNAs, suggesting its crucial role in regulating gene expression in UM. The
300 results are consistent with previous findings that SOX10 is an important TF involved in cancer
301 (15, 37) and other human pathologies (4).

302

303 **SOX10 knockdown leads to altered regulatory landscape in UM**

304 Gene regulation encompasses a complex network of mechanisms that extend far beyond
305 simple up- or down-regulation of mRNA or protein abundance (68, 69), so the change in
306 expression levels does not fully reflect the importance of genes' regulatory activities. Here, we
307 used a network method to identify crucial genes, especially miRNAs, in SOX10-KD UM cells.

308 Specifically, we first computed genes' activity based on their expression profiles and regulatory
309 interactions in a UM network developed by us and then we inferred genes with differential
310 activities in SOX10-KD UM. The results show 168 and 174 protein-coding and miRNA genes
311 with significantly upregulated and downregulated activities in SOX10-KD UM cells, respectively
312 (Figure 2B and SM Excel S3). Among these genes, SOX10's expression level and regulatory
313 activity are significantly reduced in SOX10-KD UM cells consistent with our expectation (Figure
314 2C), demonstrating the method's power to identify crucial genes in the UM network. As a
315 transcriptional activator of many genes including TFs, SOX10-KD significantly downregulates
316 several TFs' expression in UM cells, including MITF (log2FC = -2.60; adjusted p-value = 2.95E-
317 16), EDNRB (log2FC = -1.54; adjusted p-value = 1.81E-11), GJB1 (a.k.a. CX32; log2FC = -
318 3.48; adjusted p-value = 2.1E-7), and MIA (log2FC = -1.21; adjusted p-value = 0.016). These
319 alternations could drive a phenotype switch in UM. For instance, the disrupted SOX10-MITF
320 pathway may lead to reduced cell proliferation, cell cycle arrest, and increased apoptosis (70,
321 71). The diminishment of transcriptional activity for key regulatory genes EDNRB (72, 73) and
322 MIA (74) can affect cell migration, proliferation, and survival. Additionally, downregulation of
323 GJB1 is often linked to increased melanoma cell invasiveness, reduced cell adhesion, and
324 disruption of normal cellular signaling pathways that restrict tumor growth (75).

325 Our data show that GATA2, TRIM33, and PMEPA1 exhibit the most significant increase in
326 regulatory activity, while MYBL2, NEDD4L, and STUB1 exhibit the most substantial decrease
327 in regulatory activity. All six genes have been extensively studied in cutaneous melanoma but
328 not in UM. Given the similarities in melanocytic tumor biology between cutaneous melanoma
329 and UM, it is plausible that these genes play a similar role in UM. Particularly, GATA2
330 deficiency often due to epigenetic silencing is associated with an increased risk of melanoma
331 (76). TRIM33 plays dual role – tumor suppressor and oncogene - in cancers (77, 78), but its
332 relevance to melanoma remains unclear. PMEPA1 can promote tumorigenic traits in
333 melanoma, with its expression fine-tuned by RNA-binding proteins or miRNAs to drive the
334 tumor progression (79). MYBL2 is widely expressed in proliferating cells, and its aberrant
335 expression contributes to tumor malignancy and poor prognosis in melanoma patients (80).
336 MYBL2 promotes the formation of stem-like cell populations in melanoma (80). The
337 ubiquitination activity of NEDD4 is closely linked to melanoma progression (81–83). For
338 instance, disrupting NEDD4 activity stabilizes the tumor suppressor PTEN and inhibits
339 melanoma cell proliferation (84, 85). Moreover, NEDD4 positively regulates expression of
340 SOX10 (86). STUB1 regulates immune response and resistance to immunotherapy in
341 melanoma (87, 88).

342 Besides protein-coding genes, we identified 17 miRNAs with significant differential activities.
343 miR-146a-5p, miR-25-3p, and miR-34a-5p show the highest upregulated activity levels, and
344 miR-573, miR-4426, and miR-4485-5p show the greatest downregulated activity levels.

345 Notably, the regulatory activities of miRNAs successfully distinguished SOX10-KD cells from
346 controls, which was not achievable using expression profiles alone, indicating that SOX10-KD
347 reshapes miRNA regulatory networks in UM (Figure 2D).

348 Taken together, integrating gene expression profiles with the UM network enabled us to
349 characterize genes' regulatory activities in SOX10-KD UM cells, thereby identifying driver
350 miRNAs that lack significant changes in their expression levels.

351

352 **Quantification of driver miRNAs' regulatory activities**

353 To better understand the role of the identified 17 miRNAs in UM, we modeled the expression
354 patterns of these miRNAs and their target genes using NetBID2 to quantify changes in
355 miRNAs' regulatory activities (see Methods for details). Since miRNAs repress their target
356 genes' expression (49), lower expression levels of miRNA target genes indicate increased
357 miRNA regulatory activity, while higher expression levels indicate decreased miRNA regulatory
358 activity (Figure 3A).

359 Among the identified driver miRNAs, miR-146a-5p, miR-25-3p, miR-186-5p, and miR-34a-5p
360 have numerous target genes (from 10 to 77) in the UM network, suggesting their broad
361 regulatory function in UM. For instance, 54 of the 77 target genes of miR-34a-5p have
362 significantly lower expression levels in SOX10-KD UM, resulting in a strong increase in its
363 regulatory activity (Figure 3B). The significant change in regulatory activity and the large
364 number of target genes of miR-34a-5p suggest that it plays a pivotal role in controlling the cell
365 cycle, proliferation, and apoptosis in SOX10-KD UM. For instance, loss of SOX10 in melanoma
366 is known to increase p53 pathway activity (89). Our data corroborates this, showing that
367 SOX10-KD significantly upregulates TP53 expression and activity. Concurrently, we observed
368 a significant upregulation in both the expression and activity of miR-34a-5p. This is consistent
369 with a known positive feedback loop where TP53 activates miR-34a, and miR-34a, in turn,
370 reinforces TP53 activity by suppressing its negative regulator, SIRT1 (90). Interestingly,
371 accumulation of dysfunctional or mutant TP53 protein in UM is generally associated with more
372 invasive behavior and worse prognosis (91). Therefore, our results suggest a molecular
373 mechanism through which SOX10 ablation in UM drives the switch from a proliferative to an
374 invasive cellular phenotype by activating the TP53/miR-34a/SIRT1 positive feedback loop. In
375 addition, many of miR-34a-5p's target genes are linked to UM progression. For instance, MYC
376 gene amplification is found in nearly 70% of UM cases and is associated with poor prognosis
377 (92). The overexpression of BCL2 and related proteins contributes to multidrug resistance of
378 UM cells and downregulating BCL2's expression can partially reverse the tumors' drug-
379 resistant phenotype (93). CDK4/6 has been extensively studied UM, with findings showing that
380 CDK4/6 inhibition combined with other targeted therapies such as MEK inhibitors could be a

381 promising treatment strategy for UM (94). NOTCH1 signaling plays an important role in
382 promoting proliferation, invasion, and metastasis in UM (95–98). Several studies show that
383 ARF6 can regulate UM development and growth (99, 100).

384 On the other hand, the other miRNAs have no more than five target genes in the network,
385 suggesting their specific regulatory function in UM (Figure 3B). For instance, two of the four
386 target genes of miR-211-5p have significantly higher expression levels in SOX10-KD UM,
387 leading to a decrease in its regulatory activity. The two target genes are HLA-DRB1 and IL11.
388 HLA-DRB1 is essential for presenting extracellular peptides to CD4+ T-helper cells, which is
389 crucial for initiating and sustaining adaptive immune responses against tumors (101). IL11 is
390 a cytokine that primarily acts via the JAK/STAT3 pathway, which is a central driver of cell
391 survival, proliferation, and resistance to apoptosis in cancer (102).

392 In summary, we identified driver miRNAs in UM and characterized their regulatory activities.
393 Because of the complex regulatory interactions of miRNAs in the network, we need to elucidate
394 specific miRNA-gene interactions at the pathway level to better understand their function in
395 UM.

396

397 **Understanding driver miRNAs' role at the pathway level**

398 To further elaborate the role of the identified driver miRNAs in UM, we combined pathway
399 enrichment analysis, the UM network (Figure S4), and literature search to elucidate the
400 molecular mechanisms through which these miRNAs contribute to the effects of SOX10-KD in
401 UM. This integrated approach enabled us to map miRNA-regulated genes to relevant biological
402 pathways, contextualize their interactions within the reconstructed UM regulatory network, and
403 validate their reported functions in UM biology.

404 The data shows that the identified miRNAs can regulate genes that are involved in cancer
405 hallmark terms such as G2-M checkpoint and mitotic spindle of cell cycle, mTORC1 signaling,
406 targets of E2F and MYC, and fatty acid metabolism (Figure 4). Among these miRNAs, miR-
407 34a, miR-25, and miR-186 can regulate multiple genes covering most or even all hallmark
408 terms. However other miRNAs, such as miR-3189 and miR-211, can regulate a few genes in
409 specific hallmarks. In the following, we discuss the potential role of some miRNAs in UM and
410 the complete miRNA-gene interactions in different hallmark pathways and their association
411 with UM are summarized in SM Excel S6.

412 For cell cycle, the G2-M checkpoint is frequently compromised in UM, resulting in heightened
413 genomic instability and aggressive tumor phenotypes (103). This checkpoint disruption stems
414 from mutations and dysregulation of critical cell cycle regulators, including GNA11, GNAQ,
415 CDK4, and CCND1. These molecular defects facilitate hallmark cancer characteristics in UM,

416 particularly metastatic progression and unfavorable clinical outcomes (104). Our analysis
417 reveals that CDK4 and CCND1 are commonly targeted by miR-34a in UM, while miR-25 and
418 miR-3189 respectively regulate these key cell cycle checkpoints (Figure 5). The enhanced
419 regulatory activity of these miRNAs following SOX10-KD suggests that they play a pivotal role
420 in controlling DNA damage responses and proliferative capacity in UM. On the other hand, the
421 mitotic spindle is essential for accurate chromosome segregation during cell division. In UM,
422 spindle dysfunction such as centrosome amplification promotes chromosomal instability,
423 contributing to tumor progression and metastasis (105). BIRC5 encodes survivin, a
424 chromosomal passenger complex protein essential for mitotic spindle assembly, chromosome
425 segregation, and cytokinesis, whose overexpression in UM correlates with apoptosis
426 resistance (106, 107) and poor prognosis (108). Our analysis shows that downregulated
427 BIRC5 is targeted by miR-34a-5p, whose expression and activity increase following SOX10-
428 KD, suggesting an alternative TP53-independent tumor suppressor mechanism for miR-34a in
429 UM. BCL2L11 encodes BIM, a pro-apoptotic BCL-2 family member crucial for initiating
430 apoptosis in response to mitotic stress or spindle checkpoint failure, and its upregulation in UM
431 could enable elimination of genetically unstable tumor cells with spindle defects (109). We
432 showed that upregulated BCL2L11 is targeted by miR-570-3p, which is downregulated and
433 exhibits reduced regulatory activity following SOX10-KD, indicating the oncogenic role of this
434 miRNA in UM progression.

435 mTORC1 signaling represents a fundamental driver of UM pathogenesis and disease
436 progression, with its inhibition effectively reducing tumor cell proliferation, migration, and
437 invasive potential (110, 111). SLC7A5-mediated amino acid transport sustains the metabolic
438 requirements of rapidly dividing cells by maintaining mTORC1 activation and downstream
439 anabolic pathways (112). Our findings show that SLC7A5 is regulated by miR-186-5p, whose
440 activity increases following SOX10 ablation, indicating miR-186's potential function in
441 modulating UM tumorigenicity and metabolic reprogramming through mTORC1 activation
442 (Figure 5). Additionally, BCAT1 catalyzes the conversion of branched-chain amino acids into
443 α-keto acids, generating intermediate metabolites such as leucine and α-ketoglutarate that
444 serve as mTORC1 activators (113). In cutaneous melanoma, BCAT1 depletion suppressed
445 tumor proliferation and migration while diminishing oxidative phosphorylation (114). Our data
446 indicates that SOX10-KD enhances the regulatory activities of miR-25, miR-211, and miR-
447 146a, which collectively target BCAT1, suggesting their tumor suppressive functions in UM
448 (Figure 5).

449 Fatty acid metabolism is crucial in UM development and progression (115), with UM cells
450 exhibiting higher polyunsaturated fatty acid proportions than normal uveal melanocytes,
451 contributing to abnormal proliferation and altered antioxidant status (116). FASN, which
452 mediates de novo fatty acid synthesis and is upregulated in metastatic UM to support tumor

453 growth (115), is targeted by miR-186-5p whose expression and regulatory activity increase
454 following SOX10-KD, suggesting an anti-cancer role for this miRNA in regulating UM fatty
455 acid metabolism (Figure 5).

456 Taken together, our analysis reveals that SOX10-KD in UM modulates multiple miRNAs that
457 regulate hallmark pathways, including cell cycle, mTORC1 signaling, and fatty acid
458 metabolism. These miRNAs, particularly miR-34a, miR-25, miR-186, and miR-211, show
459 tumor suppressive potential by targeting genes involved in UM progression and metastasis.
460 The coordinate regulation of these pathways suggests a complex regulatory network where
461 SOX10 loss triggers compensatory tumor suppressive mechanisms through miRNA-
462 mediated pathway modulation.

463 **Discussion and conclusion**

464 This study represents the first systematic investigation into how SOX10 expression modulates
465 miRNA activity in UM. We employed a comprehensive systems biology approach to elucidate
466 the regulatory functions of miRNAs following SOX10-KD, integrating miRNA and mRNA
467 expression profiles with network modeling to conduct systematic analysis of miRNA-gene
468 interactions specific to SOX10 depletion in UM. Our network-based methodology introduces
469 an advanced perspective by demonstrating that miRNAs can exert significant regulatory
470 effects even without substantial fold-changes in their expression levels. This approach enabled
471 identification of miRNAs exhibiting significant activity changes following SOX10-KD, revealing
472 their target genes within the UM regulatory network. Functional enrichment analysis
473 demonstrated that these target genes are significantly overrepresented in critical cancer
474 hallmark pathways, which collectively regulate tumor progression through modulation of cell
475 cycle and metabolism. These findings provide mechanistic insights into pathway-level miRNA
476 functions that are influenced by SOX10's activity in UM. While the literature supports the
477 biological plausibility of our predicted miRNA-gene interactions and their associated molecular
478 mechanisms, though not all specifically in UM but in other cancers, we propose experimental
479 validation to test relevant hypotheses and validate our predictions in UM.

480 Many genes function as hidden drivers in cancer progression, exerting regulatory influence
481 without exhibiting detectable genetic alterations, epigenetic modifications, or significant
482 differential expression at the mRNA or protein levels. These hidden drivers may contribute to
483 tumor progression through mechanisms such as post-translational modifications (117),
484 epistatic gene interactions (118), or epigenetic tuning (119) that remain undetected by
485 conventional analytical approaches. Traditional genome-wide differential gene expression
486 analyses are limited in their ability to identify hidden regulators due to their reliance on the
487 magnitude of molecular changes, such as gene expression levels. To overcome this challenge,
488 we employed NetBID2, an algorithm that identifies prominent miRNAs using an informatics
489 approach to infer regulatory activity changes by integrating miRNA expression levels with
490 those of their target genes. This approach represents a paradigm shift from conventional
491 methodologies that typically identify significantly differentially expressed genes first and
492 subsequently construct networks from these candidates. Instead, we used a reverse strategy
493 by initiating our analysis with a curated network that captures consensus molecular interactions
494 for UM. This network provides a biologically informed foundation that enables more accurate
495 and contextually relevant calculation of miRNA regulatory activity in UM, potentially revealing
496 hidden regulatory mechanisms that would otherwise remain undetected through traditional
497 expression-based approaches.

498 While our approach provides several methodological advantages, certain limitations must be
499 acknowledged. Though effective, the method used to detect miRNA-gene interactions within
500 the UM network may generate false positive predictions due to bioinformatics challenges, such
501 as the minimal biological impact and non-functional conservation of miRNAs (120), as well as
502 the intricacy of miRNA-gene interactions (121). This could potentially lead to the identification
503 of spurious regulatory relationships. For example, miR-34a's repression efficacy is determined
504 by the structural and biophysical characteristics of its binding sites in the 3' UTR of the target
505 mRNA and AGO2, which can increase or decrease the binding strength of miRNAs (122).
506 Seedless binding in miR-155 and miR-124 can also lead to gene repression (123). Additionally,
507 the accuracy and reliability of NetBID2 may be constrained by our relatively small sample size,
508 which could impact both the comprehensiveness of detected interactions and the statistical
509 robustness of our findings. For example, the computed changes in miRNA regulatory activity
510 in our dataset are modest in magnitude. Despite these constraints, our work presents a
511 systematic approach for elucidating complex miRNA regulatory networks in UM. To encourage
512 reuse and reproduction of our results, we make the generated data and code accessible in
513 accordance with the FAIR principle (124).

Data availability

The code and data used in this work are archived in Zenodo (https://doi.org/10.5281/zenodo.17804306).

Declaration of AI usage

We utilized Claude (Sonnet 4.5) to enhance the clarity and readability of the paper.

Competing interests

C.B. reports consulting fees from BMS, Almirall Hermal, Immunocore, MSD, Novartis, Regeneron, Sanofi, Pierre Fabre; honoraria for lectures from Bristol Myers Squibb (BMS), Merck Sharpe and Dohme (MSD), Almirall Hermal, Immunocore, Novartis, Sanofi, Pierre Fabre, Leo Pharma; support for attending meetings from Pierre Fabre; participation on advisory boards of InflaRx, Miltenyi, BMS, Almirall Hermal, Immunocore, MSD, Novartis, Regeneron, Sanofi, Pierre Fabre outside the submitted work. C.B. is a board member of the Dermatologic Cooperative Oncology group (DeCOG). M.V.H. received honoraria for lectures and presentations from Novartis, BMS, MSD, and Immunocore and participated on data safety monitoring boards or advisory boards of Novartis, BMS, MSD, and Immunocore. The other authors declare no conflict of interest.

Acknowledgements

JV and XL were supported by the German Ministry of Education and Research (BMBF) through the project e:Med MelAutim [01ZX1905A]. J.V. was also supported by and the Masterplan Bayern Digital II [MED-1810-0023], the Manfred-Roth-Stiftung, Forschungsstiftung Medizin Uniklinikum Erlangen, and EU through the Horizon 2020 project CANCERNA. M.V.H. was supported by Hiege-Stiftung – die Deutsche Hautkrebsstiftung, Matthias Lackas-Stiftung, Dr. Helmut Legerlotz-Stiftung, K.L. Weigand'sche Stiftung, Else-Kröner-Fresenius Excellence Fellowship, Clinician Scientist Fellowship of the Arbeitsgemeinschaft Dermatologische Forschung (ADF). The clinical trial NCT04335890 which generated part of the sequencing data was funded by the Hasumi International Research Foundation. The funders had no role in the design of the study; in the collection, analyses, or interpretation of data; in the writing of the manuscript, or in the decision to publish the results.

Authors' contributions

Chunyan Luan: data curation; formal analysis; software; visualization; writing – original draft; writing – review and editing. **Anja Wessely**: data curation. **Zhesi Zhang:** software, visualization. **Liang Zhang**: software. **Adrian Weich:** data curation; writing – review and editing. **Christopher Lischer:** data curation. **Carola Berking**: supervision; resources; writing – review and editing. **Markus V. Heppt**: funding acquisition; writing – review and editing. **Julio Vera**: supervision; formal analysis; funding acquisition. writing – review and editing. **Xin Lai**: conceptualization; methodology; software; data curation; investigation; validation; formal analysis; supervision; funding acquisition; visualization; project administration; resources; writing – original draft; writing – review and editing.

Reference

1. Jager,M.J., Shields,C.L., Cebulla,C.M., Abdel-Rahman,M.H., Grossniklaus,H.E., Stern,M.-H., Carvajal,R.D., Belfort,R.N., Jia,R., Shields,J.A., *et al.* (2020) Uveal melanoma. *Nat. Rev. Dis. Primer*, **6**, 24.
2. Ali,Z., Yousaf,N. and Larkin,J. (2013) Melanoma epidemiology, biology and prognosis. *EJC Suppl. EJC Off. J. EORTC Eur. Organ. Res. Treat. Cancer Al*, **11**, 81–91.
3. van der Kooij,M.K., Speetjens,F.M., van der Burg,S.H. and Kapiteijn,E. (2019) Uveal versus cutaneous melanoma; same origin, very distinct tumor types. *Cancers*, **11**, 845.
4. Bahmad,H.F., Thiravialingam,A., Sriganeshan,K., Gonzalez,J., Alvarez,V., Ocejo,S., Abreu,A.R., Avellan,R., Arzola,A.H., Hachem,S., *et al.* (2023) Clinical Significance of SOX10 Expression in Human Pathology. *Curr. Issues Mol. Biol.*, **45**, 10131–10158.
5. Haldin,C.E. and LaBonne,C. (2010) SoxE factors as multifunctional neural crest regulatory factors. *Int. J. Biochem. Cell Biol.*, **42**, 441–444.
6. Han,S., Ren,Y., He,W., Liu,H., Zhi,Z., Zhu,X., Yang,T., Rong,Y., Ma,B., Purwin,T.J., *et al.* (2018) ERK-mediated phosphorylation regulates SOX10 sumoylation and targets expression in mutant BRAF melanoma. *Nat. Commun.*, **9**, 28.
7. Graf,S.A., Busch,C., Bosserhoff,A.-K., Besch,R. and Berking,C. (2014) SOX10 promotes melanoma cell invasion by regulating melanoma inhibitory activity. *J. Invest. Dermatol.*, **134**, 2212–2220.
8. Cronin,J.C., Watkins-Chow,D.E., Incao,A., Hasskamp,J.H., Schönewolf,N., Aoude,L.G., Hayward,N.K., Bastian,B.C., Dummer,R., Loftus,S.K., *et al.* (2013) SOX10 ablation arrests cell cycle, induces senescence, and suppresses melanomagenesis. *Cancer Res.*, **73**, 5709–5718.
9. Shakhova,O., Zingg,D., Schaefer,S.M., Hari,L., Civenni,G., Blunschi,J., Claudinot,S., Okoniewski,M., Beermann,F., Mihic-Probst,D., *et al.* (2012) Sox10 promotes the formation and maintenance of giant congenital naevi and melanoma. *Nat. Cell Biol.*, **14**, 882–890.
10. Alghamdi,S.A., Zoroquiain,P., Dias,A.B.T., Alhumaid,S.R., Aldrees,S. and Burnier,M.N. (2015) Diagnostic value of SOX-10 immunohistochemical staining for the detection of uveal melanoma. *Ecancermedicalscience*, **9**, 566.
11. Mori,T., Sukeda,A., Sekine,S., Shibata,S., Ryo,E., Okano,H., Suzuki,S. and Hiraoka,N. (2017) SOX10 Expression as Well as BRAF and GNAQ/11 Mutations Distinguish Pigmented Ciliary Epithelium Neoplasms From Uveal Melanomas. *Invest. Ophthalmol. Vis. Sci.*, **58**, 5445–5451.
12. Das,D., Kaur,I., Ali,M.J., Biswas,N.K., Das,S., Kumar,S., Honavar,S.G., Maitra,A., Chakrabarti,S. and Majumder,P.P. (2014) Exome sequencing reveals the likely involvement of SOX10 in uveal melanoma. *Optom. Vis. Sci. Off. Publ. Am. Acad. Optom.*, **91**, e185-192.
13. Ding,X., Wang,L., Chen,M., Wu,Y., Ge,S., Li,J., Fan,X. and Lin,M. (2021) Sperm-Specific Glycolysis Enzyme Glyceraldehyde-3-Phosphate Dehydrogenase Regulated by Transcription Factor SOX10 to Promote Uveal Melanoma Tumorigenesis. *Front. Cell Dev. Biol.*, **9**, 610683.
14. Centore,R.C., Soares,L.M.M., Topal,S., Vaswani,R.G., Ichikawa,K., Li,Z., Fan,H., Setser,J.W., Lahr,D.L., Zawadzke,L.E., *et al.* (2024) Pharmacologic inhibition of BAF chromatin remodeling complexes as a therapeutic approach to transcription factor-dependent cancers. *eLife*, **13**.
15. Yu,L., Peng,F., Dong,X., Chen,Y., Sun,D., Jiang,S. and Deng,C. (2020) Sex-Determining Region Y Chromosome-Related High-Mobility-Group Box 10 in Cancer: A Potential Therapeutic Target. *Front. Cell Dev. Biol.*, **8**, 564740.
16. Bartel,D.P. (2009) MicroRNAs: target recognition and regulatory functions. *Cell*, **136**, 215–233.
17. Bartel,D.P. (2018) Metazoan MicroRNAs. *Cell*, **173**, 20–51.
18. Lai,X., Schmitz,U., Gupta,S.K., Bhattacharya,A., Kunz,M., Wolkenhauer,O. and Vera,J. (2012) Computational analysis of target hub gene repression regulated by multiple and cooperative miRNAs. *Nucleic Acids Res.*, **40**, 8818–8834.
19. Panda,A.C. (2018) Circular RNAs Act as miRNA Sponges. *Adv. Exp. Med. Biol.*, **1087**, 67–79.
20. Dudekula,D.B., Panda,A.C., Grammatikakis,I., De,S., Abdelmohsen,K. and Gorospe,M. (2016) CircInteractome: A web tool for exploring circular RNAs and their interacting proteins and microRNAs. *RNA Biol.*, **13**, 34–42.
21. Conn,V.M., Chinnaiyan,A.M. and Conn,S.J. (2024) Circular RNA in cancer. *Nat. Rev. Cancer*, **24**, 597–613.
22. Wróblewska,J.P., Lach,M.S., Ustaszewski,A., Kulcenty,K., Ibbs,M., Jagiełło,I., Suchorska,W.M. and Marszałek,A. (2020) The potential role of selected miRNA in uveal melanoma primary tumors as early biomarkers of disease progression. *Genes*, **11**, 271.
23. Li,Z., Yu,X., Shen,J. and Jiang,Y. (2015) MicroRNA dysregulation in uveal melanoma: a new player enters the game. *Oncotarget*, **6**, 4562–4568.
24. Yang,C., Wang,Y. and Hardy,P. (2021) Emerging roles of microRNAs and their implications in uveal melanoma. *Cell. Mol. Life Sci. CMLS*, **78**, 545–559.

25. Li,Y.F., Dong,L., Li,Y. and Wei,W.B. (2020) A Review of MicroRNA in Uveal Melanoma. *OncoTargets Ther.*, **13**, 6351–6359.
26. Lai,X., Wolkenhauer,O. and Vera,J. (2016) Understanding microRNA-mediated gene regulatory networks through mathematical modelling. *Nucleic Acids Res.*, **44**, 6019–6035.
27. Zhang,L., He,X., Li,F., Pan,H., Huang,X., Wen,X., Zhang,H., Li,B., Ge,S., Xu,X., *et al.* (2018) The miR-181 family promotes cell cycle by targeting CTDSPL, a phosphatase-like tumor suppressor in uveal melanoma. *J. Exp. Clin. Cancer Res. CR*, **37**, 15.
28. Zhang,C. and Wu,S. (2024) ZNF197-AS1/miR-425/GABARAPL1 axis: a novel regulatory mechanism in uveal melanoma. *Am. J. Physiol. Cell Physiol.*, **327**, C1638–C1650.
29. Hou,Q., Han,S., Yang,L., Chen,S., Chen,J., Ma,N., Wang,C., Tang,J., Chen,X., Chen,F., *et al.* (2019) The Interplay of MicroRNA-34a, LGR4, EMT-Associated Factors, and MMP2 in Regulating Uveal Melanoma Cells. *Invest. Ophthalmol. Vis. Sci.*, **60**, 4503–4510.
30. Venkatesan,N., Kanwar,J., Deepa,P.R., Khetan,V., Crowley,T.M., Raguraman,R., Sugneswari,G., Rishi,P., Natarajan,V., Biswas,J., *et al.* (2016) Clinico-Pathological Association of Delineated miRNAs in Uveal Melanoma with Monosomy 3/Disomy 3 Chromosomal Aberrations. *PloS One*, **11**, e0146128.
31. Falzone,L., Romano,G.L., Salemi,R., Bucolo,C., Tomasello,B., Lupo,G., Anfuso,C.D., Spandidos,D.A., Libra,M. and Candido,S. (2019) Prognostic significance of deregulated microRNAs in uveal melanomas. *Mol. Med. Rep.*, **19**, 2599–2610.
32. Wróblewska,J.P., Lach,M.S., Ustaszewski,A., Kulcenty,K., Ibbs,M., Jagiełło,I., Suchorska,W.M. and Marszałek,A. (2020) The Potential Role of Selected miRNA in Uveal Melanoma Primary Tumors as Early Biomarkers of Disease Progression. *Genes*, **11**, 271.
33. Xin,X., Zhang,Y., Ling,F., Wang,L., Sheng,X., Qin,L. and Zhao,X. (2019) Identification of a nine-miRNA signature for the prognosis of Uveal Melanoma. *Exp. Eye Res.*, **180**, 242–249.
34. Yang,C., Wang,R. and Hardy,P. (2021) Potential of miRNA-Based Nanotherapeutics for Uveal Melanoma. *Cancers*, **13**, 5192.
35. Lai,X., Eberhardt,M., Schmitz,U. and Vera,J. (2019) Systems biology-based investigation of cooperating microRNAs as monotherapy or adjuvant therapy in cancer. *Nucleic Acids Res.*, **47**, 7753–7766.
36. Lai,X., Gupta,S.K., Schmitz,U., Marquardt,S., Knoll,S., Spitschak,A., Wolkenhauer,O., Pützer,B.M. and Vera,J. (2018) MiR-205-5p and miR-342-3p cooperate in the repression of the E2F1 transcription factor in the context of anticancer chemotherapy resistance. *Theranostics*, **8**, 1106–1120.
37. Lai,X., Luan,C., Zhang,Z., Wessely,A., Heppt,M.V., Berking,C. and Vera,J. (2025) SOX10, MITF, and microRNAs: Decoding their interplay in regulating melanoma plasticity. *Int. J. Cancer*, 10.1002/ijc.35499.
38. Purwin,T.J., Caksa,S., Sacan,A., Capparelli,C. and Aplin,A.E. (2023) Gene signature reveals decreased SOX10-dependent transcripts in malignant cells from immune checkpoint inhibitor-resistant cutaneous melanomas. *iScience*, **26**, 107472.
39. Capparelli,C., Purwin,T.J., Glasheen,M., Caksa,S., Tiago,M., Wilski,N., Pomante,D., Rosenbaum,S., Nguyen,M.Q., Cai,W., *et al.* (2022) Targeting SOX10-deficient cells to reduce the dormant-invasive phenotype state in melanoma. *Nat. Commun.*, **13**, 1381.
40. Graf,S.A., Heppt,M.V., Wessely,A., Krebs,S., Kammerbauer,C., Hornig,E., Strieder,A., Blum,H., Bosserhoff,A.-K. and Berking,C. (2019) The myelin protein PMP2 is regulated by SOX10 and drives melanoma cell invasion. *Pigment Cell Melanoma Res.*, **32**, 424–434.
41. Wessely,A., Lischer,C., Weich,A., Kammerbauer,C., Güse,E., Koch,E.A.T., Lai,X., Dörrie,J., Erdmann,M., Voskens,C., *et al.* (2025) A computational SOX10 network-based selection strategy to identify new drug targets in uveal melanoma. 10.1101/2025.10.14.679939.
42. Frankish,A., Diekhans,M., Jungreis,I., Lagarde,J., Loveland,J.E., Mudge,J.M., Sisu,C., Wright,J.C., Armstrong,J., Barnes,I., *et al.* (2021) Gencode 2021. *Nucleic Acids Res.*, **49**, D916–D923.
43. Dobin,A., Davis,C.A., Schlesinger,F., Drenkow,J., Zaleski,C., Jha,S., Batut,P., Chaisson,M. and Gingeras,T.R. (2013) STAR: ultrafast universal RNA-seq aligner. *Bioinforma. Oxf. Engl.*, **29**, 15–21.
44. Ewels,P., Magnusson,M., Lundin,S. and Käller,M. (2016) MultiQC: summarize analysis results for multiple tools and samples in a single report. *Bioinforma. Oxf. Engl.*, **32**, 3047–3048.
45. Kozomara,A., Birgaoanu,M. and Griffiths-Jones,S. (2019) miRBase: from microRNA sequences to function. *Nucleic Acids Res.*, **47**, D155–D162.
46. Johnson,W.E., Li,C. and Rabinovic,A. (2007) Adjusting batch effects in microarray expression data using empirical Bayes methods. *Biostat. Oxf. Engl.*, **8**, 118–127.
47. Du,X., Wen,J., Wang,Y., Karmaus,P.W.F., Khatamian,A., Tan,H., Li,Y., Guy,C., Nguyen,T.-L.M., Dhungana,Y., *et al.* (2018) Hippo/Mst signalling couples metabolic state and immune function of CD8α+ dendritic cells. *Nature*, **558**, 141–145.
48. Dong,X., Ding,L., Thrasher,A., Wang,X., Liu,J., Pan,Q., Rash,J., Dhungana,Y., Yang,X., Risch,I., *et al.* (2023) NetBID2 provides comprehensive hidden driver analysis. *Nat. Commun.*, **14**, 2581.

677 49. Bartel,D.P. (2018) Metazoan MicroRNAs. *Cell*, **173**, 20–51.
678 50. Evangelista,J.E., Xie,Z., Marino,G.B., Nguyen,N., Clarke,D.J.B. and Ma'ayan,A. (2023) Enrichr-
679 KG: bridging enrichment analysis across multiple libraries. *Nucleic Acids Res.*, **51**, W168–W179.
680 51. Liberzon,A., Birger,C., Thorvaldsdóttir,H., Ghandi,M., Mesirov,J.P. and Tamayo,P. (2015) The
681 Molecular Signatures Database (MSigDB) hallmark gene set collection. *Cell Syst.*, **1**, 417–425.
682 52. Fuchs,R.T., Sun,Z., Zhuang,F. and Robb,G.B. (2015) Bias in ligation-based small RNA
683 sequencing library construction is determined by adaptor and RNA structure. *PloS One*, **10**, e0126049.
684 53. Kozubek,J., Ma,Z., Fleming,E., Duggan,T., Wu,R., Shin,D.-G. and Dadras,S.S. (2013) In-depth
685 characterization of microRNA transcriptome in melanoma. *PloS One*, **8**, e72699.
686 54. Chan,E., Patel,R., Nallur,S., Ratner,E., Bacchiocchi,A., Hoyt,K., Szpakowski,S., Godshalk,S.,
687 Ariyan,S., Sznol,M., *et al.* (2011) MicroRNA signatures differentiate melanoma subtypes. *Cell Cycle*
688 *Georget. Tex*, **10**, 1845–1852.
689 55. Gramantieri,L., Fornari,F., Ferracin,M., Veronese,A., Sabbioni,S., Calin,G.A., Grazi,G.L.,
690 Croce,C.M., Bolondi,L. and Negrini,M. (2009) MicroRNA-221 targets Bmf in hepatocellular carcinoma
691 and correlates with tumor multifocality. *Clin. Cancer Res. Off. J. Am. Assoc. Cancer Res.*, **15**, 5073–
692 5081.
693 56. Fan,Y.-X., Bian,X.-H., Qian,P.-D., Chen,Z.-Z., Wen,J., Luo,Y.-H., Yan,P.-W. and Zhang,Q. (2018)
694 MicroRNA-125b inhibits cell proliferation and induces cell apoptosis in esophageal squamous cell
695 carcinoma by targeting BMF. *Oncol. Rep.*, **40**, 61–72.
696 57. Cheng,H., Chua,V., Liao,C., Purwin,T.J., Terai,M., Kageyama,K., Davies,M.A., Sato,T. and
697 Aplin,A.E. (2017) Co-targeting HGF/cMET Signaling with MEK Inhibitors in Metastatic Uveal
698 Melanoma. *Mol. Cancer Ther.*, **16**, 516–528.
699 58. Schoumacher,M., Le Corre,S., Houy,A., Mulugeta,E., Stern,M.-H., Roman-Roman,S. and
700 Margueron,R. (2016) Uveal melanoma cells are resistant to EZH2 inhibition regardless of BAP1
701 status. *Nat. Med.*, **22**, 577–578.
702 59. Yu,J., Wu,X., Yan,J., Yu,J., Yin,T., Dai,J., Ma,M., Xu,T., Yu,H., Xu,L., *et al.* (2019) Potential
703 Mutations in Uveal Melanoma Identified Using Targeted Next-Generation Sequencing. *J. Cancer*, **10**,
704 488–493.
705 60. Singhal,R., Bard,J.E., Nowak,N.J., Buck,M.J. and Kandel,E.S. (2013) FOXO1 regulates
706 expression of a microRNA cluster on X chromosome. *Aging*, **5**, 347–356.
707 61. Song,Z., Shao,W., Xiahou,Z., Xu,Y. and Zhang,X. (2024) Single-cell RNA sequencing reveals key
708 molecular drivers and immune landscape in uveal melanoma: implications for targeted therapy and
709 prognostic modeling. *Front. Immunol.*, **15**, 1493752.
710 62. Yang,F., Li,L., Mu,Z., Liu,P., Wang,Y., Zhang,Y. and Han,X. (2022) Tumor-promoting properties of
711 karyopherin β1 in melanoma by stabilizing Ras-GTPase-activating protein SH3 domain-binding protein
712 1. *Cancer Gene Ther.*, **29**, 1939–1950.
713 63. Lara-Lemus,R., Castillejos-López,M. and Aquino-Gálvez,A. (2024) The Possible Roles of
714 Glucosamine-6-Phosphate Deaminases in Ammonium Metabolism in Cancer. *Int. J. Mol. Sci.*, **25**,
715 12054.
716 64. Sun,B. and Zhao,H. (2021) The bioinformatics analysis of RIOX2 gene in lung adenocarcinoma
717 and squamous cell carcinoma. *PloS One*, **16**, e0259447.
718 65. He,C., Liu,W., Sun,J., Zhang,D. and Li,B. (2023) Jumonji domain-containing protein RIOX2 is
719 overexpressed and associated with worse survival outcomes in prostate cancers. *Front. Oncol.*, **13**,
720 1087082.
721 66. Ding,Z., Jian,S., Peng,X., Liu,Y., Wang,J., Zheng,L., Ou,C., Wang,Y., Zeng,W. and Zhou,M.
722 (2015) Loss of MiR-664 Expression Enhances Cutaneous Malignant Melanoma Proliferation by
723 Upregulating PLP2. *Medicine (Baltimore)*, **94**, e1327.
724 67. Hong,H., Yao,S., Zhang,Y., Ye,Y., Li,C., Hu,L., Sun,Y., Huang,H.-Y. and Ji,H. (2020) In vivo
725 miRNA knockout screening identifies miR-190b as a novel tumor suppressor. *PLoS Genet.*, **16**,
726 e1009168.
727 68. Davidson,E. and Levin,M. (2005) Gene regulatory networks. *Proc. Natl. Acad. Sci. U. S. A.*, **102**,
728 4935.
729 69. Zhao,M., He,W., Tang,J., Zou,Q. and Guo,F. (2021) A comprehensive overview and critical
730 evaluation of gene regulatory network inference technologies. *Brief. Bioinform.*, **22**, bbab009.
731 70. Tudrej,K.B., Czepielewska,E. and Kozłowska-Wojciechowska,M. (2017) SOX10-MITF pathway
732 activity in melanoma cells. *Arch. Med. Sci. AMS*, **13**, 1493–1503.
733 71. Kawakami,A. and Fisher,D.E. (2017) The master role of microphthalmia-associated transcription
734 factor in melanocyte and melanoma biology. *Lab. Investig. J. Tech. Methods Pathol.*, **97**, 649–656.
735 72. Yokoyama,S., Takeda,K. and Shibahara,S. (2006) SOX10, in combination with Sp1, regulates the
736 endothelin receptor type B gene in human melanocyte lineage cells. *FEBS J.*, **273**, 1805–1820.

73. Zhu,L., Lee,H.-O., Jordan,C.S., Cantrell,V.A., Southard-Smith,E.M. and Shin,M.K. (2004) Spatiotemporal regulation of endothelin receptor-B by SOX10 in neural crest-derived enteric neuron precursors. *Nat. Genet.*, **36**, 732–737.
74. Xie,W.F., Zhang,X., Sakano,S., Lefebvre,V. and Sandell,L.J. (1999) Trans-activation of the mouse cartilage-derived retinoic acid-sensitive protein gene by Sox9. *J. Bone Miner. Res. Off. J. Am. Soc. Bone Miner. Res.*, **14**, 757–763.
75. Oliveira,M.C., Verswyvel,H., Smits,E., Cordeiro,R.M., Bogaerts,A. and Lin,A. (2022) The pro- and anti-tumoral properties of gap junctions in cancer and their role in therapeutic strategies. *Redox Biol.*, **57**, 102503.
76. Nguyen,J., Alexander,T., Jiang,H., Hill,N., Abdullaev,Z., Pack,S.D., Hsu,A.P., Holland,S.M., Hickstein,D.D., Engels,E.A., *et al.* (2018) Melanoma in patients with GATA2 deficiency. *Pigment Cell Melanoma Res.*, **31**, 337–340.
77. Wang,F., Wang,W., Wu,X., Tang,C., Du,F., Lu,Z., Zhang,Z., Xu,H., Cao,X. and Li,P.A. (2022) Downregulation of TRIM33 Promotes Survival and Epithelial-Mesenchymal Transition in Gastric Cancer. *Technol. Cancer Res. Treat.*, **21**, 15330338221114505.
78. Xia,T., Meng,L., Xu,G., Sun,H. and Chen,H. (2024) TRIM33 promotes glycolysis through regulating P53 K48-linked ubiquitination to promote esophageal squamous cell carcinoma growth. *Cell Death Dis.*, **15**, 740.
79. Kakumani,P.K., Guitart,T., Houle,F., Harvey,L.-M., Goyer,B., Germain,L., Gebauer,F. and Simard,M.J. (2021) CSDE1 attenuates microRNA-mediated silencing of PMEPA1 in melanoma. *Oncogene*, **40**, 3231–3244.
80. Zhong,F., Liu,J., Gao,C., Chen,T. and Li,B. (2022) Downstream regulatory network of MYBL2 mediating its oncogenic role in melanoma. *Front. Oncol.*, **12**, 816070.
81. Guo,Y., Yang,L., Lei,S., Tan,W. and Long,J. (2019) NEDD4 negatively regulates GITR via ubiquitination in immune microenvironment of melanoma. *OncoTargets Ther.*, **12**, 10629–10637.
82. Lévy,F., Muehlethaler,K., Salvi,S., Peitrequin,A.-L., Lindholm,C.K., Cerottini,J.-C. and Rimoldi,D. (2005) Ubiquitylation of a melanosomal protein by HECT-E3 ligases serves as sorting signal for lysosomal degradation. *Mol. Biol. Cell*, **16**, 1777–1787.
83. Cui,J., Shu,C., Xu,J., Chen,D., Li,J., Ding,K., Chen,M., Li,A., He,J., Shu,Y., *et al.* (2020) JP1 suppresses proliferation and metastasis of melanoma through MEK1/2 mediated NEDD4L-SP1-integrin αvβ3 signaling. *Theranostics*, **10**, 8036–8050.
84. Aronchik,I., Kundu,A., Quirit,J.G. and Firestone,G.L. (2014) The antiproliferative response of indole-3-carbinol in human melanoma cells is triggered by an interaction with NEDD4-1 and disruption of wild-type PTEN degradation. *Mol. Cancer Res. MCR*, **12**, 1621–1634.
85. Jayaprakash,S., Hegde,M., BharathwajChetty,B., Girisa,S., Alqahtani,M.S., Abbas,M., Sethi,G. and Kunnumakkara,A.B. (2022) Unraveling the potential role of NEDD4-like E3 ligases in cancer. *Int. J. Mol. Sci.*, **23**, 12380.
86. Wiszniak,S., Kabbara,S., Lumb,R., Scherer,M., Secker,G., Harvey,N., Kumar,S. and Schwarz,Q. (2013) The ubiquitin ligase Nedd4 regulates craniofacial development by promoting cranial neural crest cell survival and stem-cell like properties. *Dev. Biol.*, **383**, 186–200.
87. Apriamashvili,G., Vredevoogd,D.W., Krijgsman,O., Bleijerveld,O.B., Ligtenberg,M.A., de Bruijn,B., Boshuizen,J., Traets,J.J.H., D'Empaire Altimari,D., van Vliet,A., *et al.* (2022) Ubiquitin ligase STUB1 destabilizes IFNγ-receptor complex to suppress tumor IFNγ signaling. *Nat. Commun.*, **13**, 1923.
88. Ng,S., Lim,S., Sim,A.C.N., Mangadu,R., Lau,A., Zhang,C., Martinez,S.B., Chandramohan,A., Lim,U.-M., Ho,S.S.W., *et al.* (2022) STUB1 is an intracellular checkpoint for interferon gamma sensing. *Sci. Rep.*, **12**, 14087.
89. Capparelli,C., Purwin,T.J., Glasheen,M., Caksa,S., Tiago,M., Wilski,N., Pomante,D., Rosenbaum,S., Nguyen,M.Q., Cai,W., *et al.* (2022) Targeting SOX10-deficient cells to reduce the dormant-invasive phenotype state in melanoma. *Nat. Commun.*, **13**, 1381.
90. Lai,X., Wolkenhauer,O. and Vera,J. (2012) Modeling miRNA regulation in cancer signaling systems: miR-34a regulation of the p53/Sirt1 signaling module. *Methods Mol. Biol. Clifton NJ*, **880**, 87–108.
91. Liu,H. and Zhou,M. (2017) Evaluation of p53 gene expression and prognosis characteristics in uveal melanoma cases. *OncoTargets Ther.*, **10**, 3429–3434.
92. Ambrosini,G. and Schwartz,G.K. (2014) Abstract 1410: gnaq/11 mutant uveal melanoma is susceptible to Brd4 inhibition by JQ1. *Cancer Res.*, **74**, 1410.
93. Guo,L., Wu,Z., Zhang,S., Zheng,J. and Zheng,H. (2003) [effect of bcl-2 antisense oligonucleotides on multidrug resistance of cultured uveal melanoma cells]. *Zhonghua Yan Ke Za Zhi Chin. J. Ophthalmol.*, **39**, 73–76.

94. Teh,J.L.F., Purwin,T.J., Han,A., Chua,V., Patel,P., Baqai,U., Liao,C., Bechtel,N., Sato,T., Davies,M.A., *et al.* (2020) Metabolic Adaptations to MEK and CDK4/6 Cotargeting in Uveal Melanoma. *Mol. Cancer Ther.*, **19**, 1719–1726.
95. Asnaghi,L., Coonfield,M.L., Schreck,K.C., Bar,E.E., Handa,J., Merbs,S., Ebrahimi,K., Harbour,J. and Eberhart,C.G. (2010) Notch signaling: a new potential target in the treatment of uveal melanoma. *Invest. Ophthalmol. Vis. Sci.*, **51**, 3803.
96. Huang,X., Wang,L., Zhang,H., Wang,H., Zhao,X., Qian,G., Hu,J., Ge,S. and Fan,X. (2012) Therapeutic efficacy by targeting correction of Notch1-induced aberrants in uveal tumors. *PloS One*, **7**, e44301.
97. Asnaghi,L., Lin,M., Lim,K., Lim,K., Bar,E. and Eberhart,C. (2013) Targeting the hypoxia pathway in uveal melanoma cells. *Acta Ophthalmol. (Copenh.)*, **91**, 0–0.
98. Asnaghi,L., Handa,J.T., Merbs,S.L., Harbour,J.W. and Eberhart,C.G. (2013) A role for Jag2 in promoting uveal melanoma dissemination and growth. *Invest. Ophthalmol. Vis. Sci.*, **54**, 295–306.
99. Yoo,J.H., Shi,D.S., Grossmann,A.H., Sorensen,L.K., Tong,Z., Mleynek,T.M., Rogers,A., Zhu,W., Richards,J.R., Winter,J.M., *et al.* (2016) ARF6 Is an Actionable Node that Orchestrates Oncogenic GNAQ Signaling in Uveal Melanoma. *Cancer Cell*, **29**, 889–904.
100. Oncogenic GNAQ Acts through a Single Node in Uveal Melanoma (2016) *Cancer Discov.*, **6**, 692.
101. Deng,H., Chen,Y., Wang,J. and An,R. (2022) HLA-DRB1: A new potential prognostic factor and therapeutic target of cutaneous melanoma and an indicator of tumor microenvironment remodeling. *PloS One*, **17**, e0274897.
102. Xu,D.H., Zhu,Z., Wakefield,M.R., Xiao,H., Bai,Q. and Fang,Y. (2016) The role of IL-11 in immunity and cancer. *Cancer Lett.*, **373**, 156–163.
103. Ortega,M.A., Fraile-Martínez,O., García-Honduvilla,N., Coca,S., Álvarez-Mon,M., Buján,J. and Teus,M.A. (2020) Update on uveal melanoma: Translational research from biology to clinical practice (Review). *Int. J. Oncol.*, **57**, 1262–1279.
104. Shao,Y.F., Baca,Y., Hinton,A., Xiu,J., VanderWalde,A., Hadfield,M., Park,S.J., Darabi,S., Sato,T. and Moser,J.C. (2025) Immune Profiling of Uveal Melanoma Liver Metastases and Response to Checkpoint Inhibitors. *J. Immunother. Hagerstown Md 1997*, **48**, 189–195.
105. Sabat-Pośpiech,D., Fabian-Kolpanowicz,K., Kalirai,H., Kipling,N., Coupland,S.E., Coulson,J.M. and Fielding,A.B. (2022) Aggressive uveal melanoma displays a high degree of centrosome amplification, opening the door to therapeutic intervention. *J. Pathol. Clin. Res.*, **8**, 383–394.
106. Li,H., Niederkorn,J.Y., Neelam,S. and Alizadeh,H. (2006) Downregulation of survivin expression enhances sensitivity of cultured uveal melanoma cells to cisplatin treatment. *Exp. Eye Res.*, **83**, 176–182.
107. Li,H., Niederkorn,J.Y., Neelam,S. and Alizadeh,H. (2005) Resistance and susceptibility of human uveal melanoma cells to TRAIL-induced apoptosis. *Arch. Ophthalmol. Chic. Ill 1960*, **123**, 654–661.
108. Fäldt Beding,A., Larsson,P., Helou,K., Einbeigi,Z. and Parris,T.Z. (2022) Pan-cancer analysis identifies BIRC5 as a prognostic biomarker. *BMC Cancer*, **22**, 322.
109. Gu,Z., Wang,X., Qi,R., Wei,L., Huo,Y., Ma,Y., Shi,L., Chang,Y., Li,G. and Zhou,L. (2015) Oridonin induces apoptosis in uveal melanoma cells by upregulation of Bim and downregulation of Fatty Acid Synthase. *Biochem. Biophys. Res. Commun.*, **457**, 187–193.
110. Banimohammad,M., Khalafi,P., Gholamin,D., Bangaleh,Z., Akhtar,N., Solomon,A.D., Prabhakar,P.K., Sanami,S., Prakash,A. and Pazoki-Toroudi,H. (2025) Exploring recent advances in signaling pathways and hallmarks of uveal melanoma: a comprehensive review. *Explor. Target. Anti-Tumor Ther.*, **6**, 1002306.
111. Geng,Y., Geng,Y., Liu,X., Chai,Q., Li,X., Ren,T. and Shang,Q. (2023) PI3K/AKT/mTOR pathway-derived risk score exhibits correlation with immune infiltration in uveal melanoma patients. *Front. Oncol.*, **13**, 1167930.
112. Hansen,C.G., Ng,Y.L.D., Lam,W.-L.M., Plouffe,S.W. and Guan,K.-L. (2015) The Hippo pathway effectors YAP and TAZ promote cell growth by modulating amino acid signaling to mTORC1. *Cell Res.*, **25**, 1299–1313.
113. Zhang,L. and Han,J. (2017) Branched-chain amino acid transaminase 1 (BCAT1) promotes the growth of breast cancer cells through improving mTOR-mediated mitochondrial biogenesis and function. *Biochem. Biophys. Res. Commun.*, **486**, 224–231.
114. Xu,E., Ji,B., Jin,K. and Chen,Y. (2023) Branched-chain amino acids catabolism and cancer progression: focus on therapeutic interventions. *Front. Oncol.*, **13**, 1220638.
115. Han,A., Mukha,D., Chua,V., Purwin,T.J., Tiago,M., Modasia,B., Baqai,U., Aumiller,J.L., Bechtel,N., Hunter,E., *et al.* (2023) Co-Targeting FASN and mTOR Suppresses Uveal Melanoma Growth. *Cancers*, **15**, 3451.

855 116. Blasi,M.A., Maresca,V., Roccella,M., Roccella,F., Sansolini,T., Grammatico,P., Balestrazzi,E. and
856 Picardo,M. (1999) Antioxidant pattern in uveal melanocytes and melanoma cell cultures. *Invest.*
857 *Ophthalmol. Vis. Sci.*, **40**, 3012–3016.
858 117. Climente-González,H., Porta-Pardo,E., Godzik,A. and Eyras,E. (2017) The Functional Impact of
859 Alternative Splicing in Cancer. *Cell Rep.*, **20**, 2215–2226.
860 118. Zhao,X., Li,J., Liu,Z. and Powers,S. (2021) Combinatorial CRISPR/Cas9 Screening Reveals
861 Epistatic Networks of Interacting Tumor Suppressor Genes and Therapeutic Targets in Human Breast
862 Cancer. *Cancer Res.*, **81**, 6090–6105.
863 119. Edrei,Y., Levy,R., Kaye,D., Marom,A., Radlwimmer,B. and Hellman,A. (2023) Methylation-
864 directed regulatory networks determine enhancing and silencing of mutation disease driver genes and
865 explain inter-patient expression variation. *Genome Biol.*, **24**, 264.
866 120. Pinzón,N., Li,B., Martinez,L., Sergeeva,A., Presumey,J., Apparailly,F. and Seitz,H. (2017)
867 microRNA target prediction programs predict many false positives. *Genome Res.*, **27**, 234–245.
868 121. Diener,C., Keller,A. and Meese,E. (2024) The miRNA-target interactions: An underestimated
869 intricacy. *Nucleic Acids Res.*, **52**, 1544–1557.
870 122. Sweetapple,L., Kosek,D.M., Banijamali,E., Becker,W., Müller,J., Karadiakos,C., Baronti,L.,
871 Guzzetti,I., Schritt,D., Chen,A., *et al.* (2025) Sequence, structure, and affinity of miR-34a binding sites
872 determine repression efficacy. *Nucleic Acids Res.*, **53**, gkaf633.
873 123. Hall,M.H., Wang,P.Y., Pham,T.M. and Bartel,D.P. (2025) Functional microRNA targeting without
874 seed pairing. *Nucleic Acids Res.*, **53**, gkaf1018.
875 124. Wilkinson,M.D., Dumontier,M., Aalbersberg,I.J.J., Appleton,G., Axton,M., Baak,A., Blomberg,N.,
876 Boiten,J.-W., da Silva Santos,L.B., Bourne,P.E., *et al.* (2016) The FAIR Guiding Principles for scientific
877 data management and stewardship. *Sci. Data*, **3**, 160018.
878

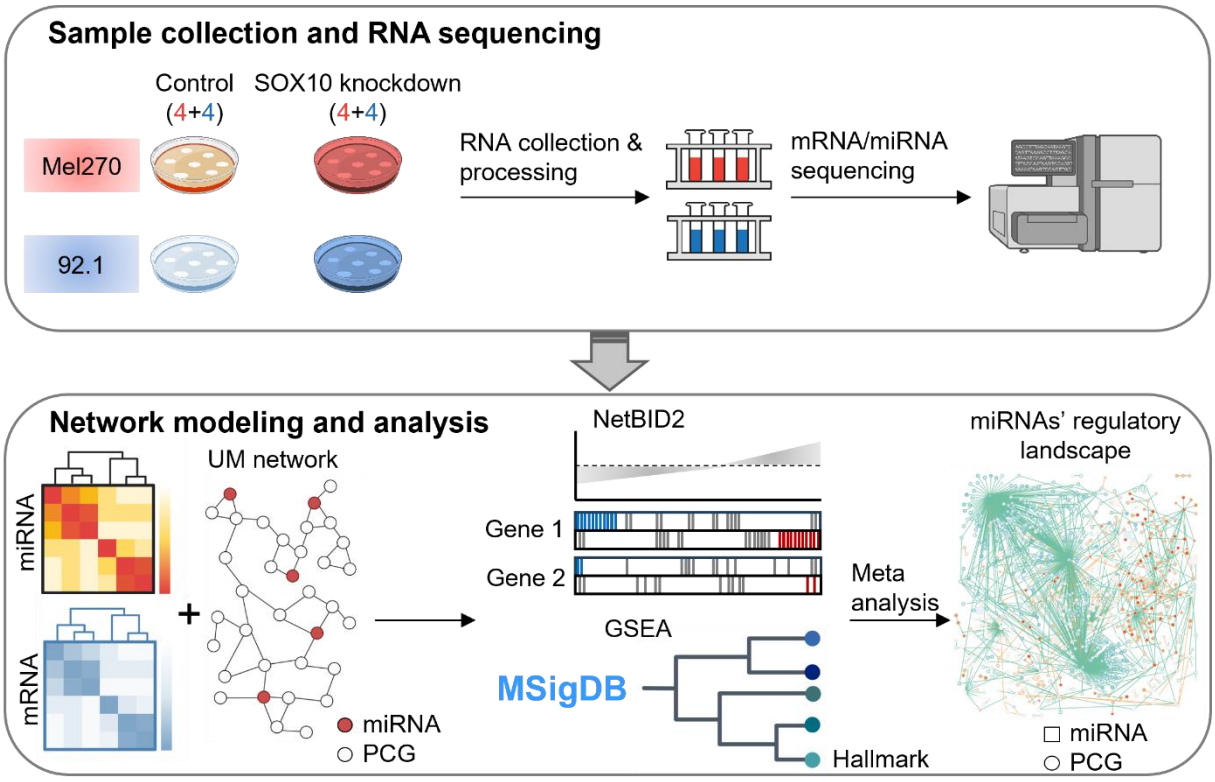

Figure 1: A network-based approach to investigate miRNA function in SOX10-KD UM cells. We began with the preparation of UM cells, where SOX10 is knocked down in the case group while the control group remains untreated. Following sample collection, we performed RNA sequencing to profile miRNA and mRNA expression levels. Subsequently, we input the data together with the network into NetBID2 that combines gene expression levels and miRNA-gene interactions to identify driver miRNAs. Finally, we performed gene set enrichment analysis (GESA) using the identified driver miRNAs' targets to elaborate their roles in UM with the help of the UM network and literature mining. The detailed computational workflow is shown in Figure S1.

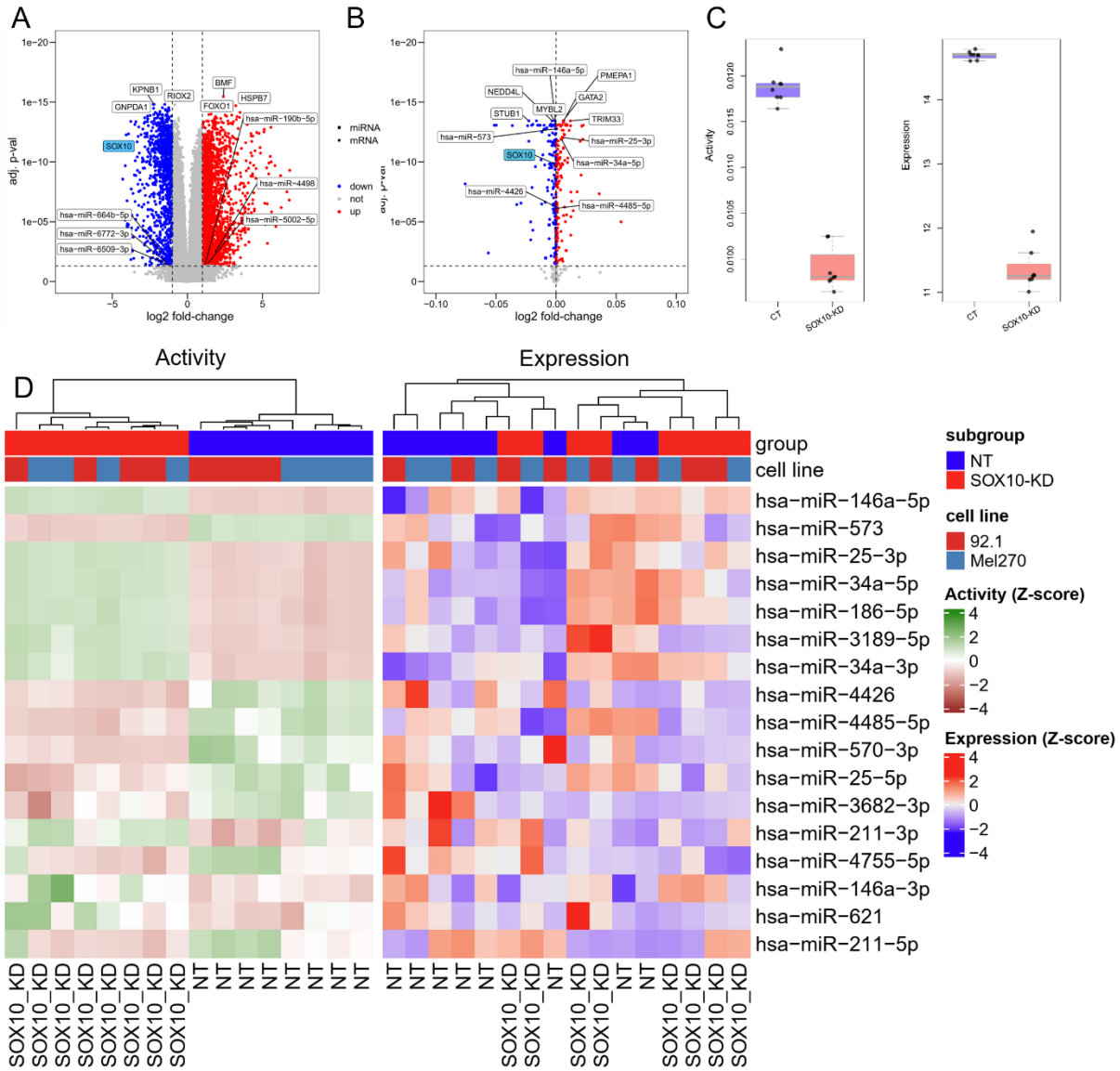

Figure 2: Differential expression and activity analysis. The volcano plots show differentially expressed genes (**A**) and genes with differentially regulatory activities (**B**) that are identified in SOX10-KD UM cells. Genes with significant change in gene expression (adjusted p-value ≤ 0.05 and |log2FC| ≥ 1) or regulatory activity (adjusted p-value ≤ 0.05) are shown in red (upregulated) and blue (downregulated), respectively. The labelled genes including protein-coding genes (square) and miRNAs (circle) are the top dysregulated ones (determined by adjusted p-value). SOX10 is highlighted in blue. (**C**) The box plot shows SOX10's expression levels and regulatory activity in SOX10-KD and control groups (CT). (**D**) The heat map shows the expression levels and regulatory activity of the identified driver miRNAs. Both data are transformed using Z-scores. The samples are hierarchically clustered using the Euclidian distance between samples.

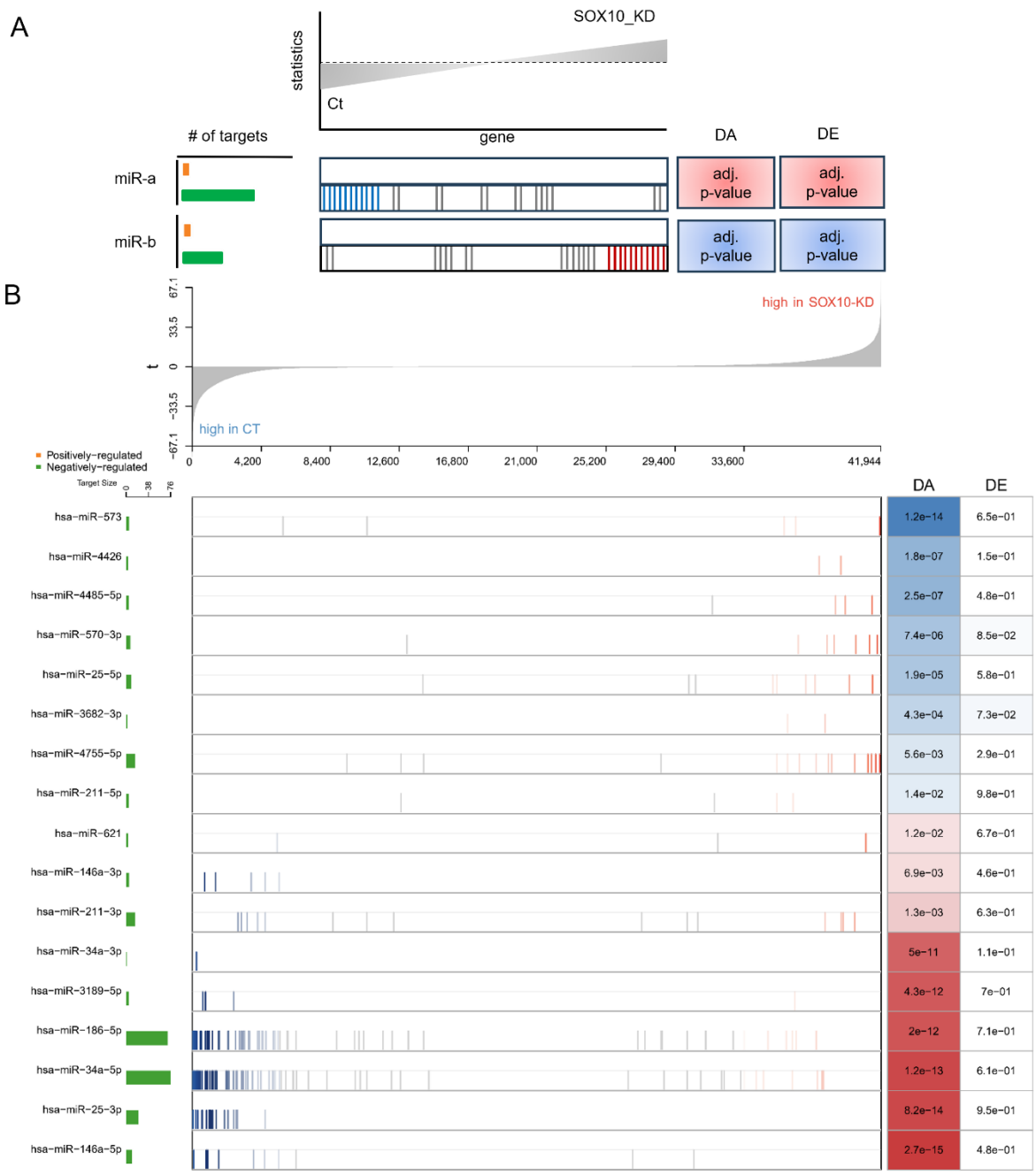

Figure 3: Regulatory profiles of the identified driver miRNAs. (**A**) The illustration of DA analysis results using NetBID2. The upper plot shows the distribution of target genes' t statistics, with genes expressing higher levels in the control group positioned on the left and genes expressing higher levels in the SOX10-KD group positioned on the right. The bottom panel provides a regulatory landscape of miRNAs. Each row represents a driver miRNA and its targets' expression profiles. Each vertical bar represents a target gene and its position that is determined by its t statistics in the upper plot. The bar in blue or red indicates whether the corresponding target gene is significantly (|z-score of t-statistics| ≥ 1.64 corresponding to p-value <= 0.10) down- or up-regulated in SOX10-KD samples, otherwise it is grey. The bar plot on the left shows the number of target genes that are positively (green) and negatively (orange) regulated by a miRNA, respectively. The orange bar is not shown (i.e. its value is zero), because miRNA-target interactions are negative regulation due to miRNA's repressive effects on target genes' expression levels. The boxes on the right show the DA and DE results of miRNAs. Blue and red boxes represent significantly (|z-score of t-statistics| ≥ 1.64 corresponding to p-value <=0.10; the darker color the higher z-score value) down- and up-regulated activity of miRNAs, respectively. The numbers in the boxes are the corresponding adjusted p-values (the false discovery rate approach). miR-a and miR-b are two examples whose regulatory activities have significantly increased and decreased due to the altered expression profiles of their target genes in SOX10-KD UM cells. (**B**) The results for the

917 identified 17 driver miRNAs. The figure has the same layout as shown in the illustration. The detailed
918 information on the driver miRNAs' target genes can be found in SM Excel S5.

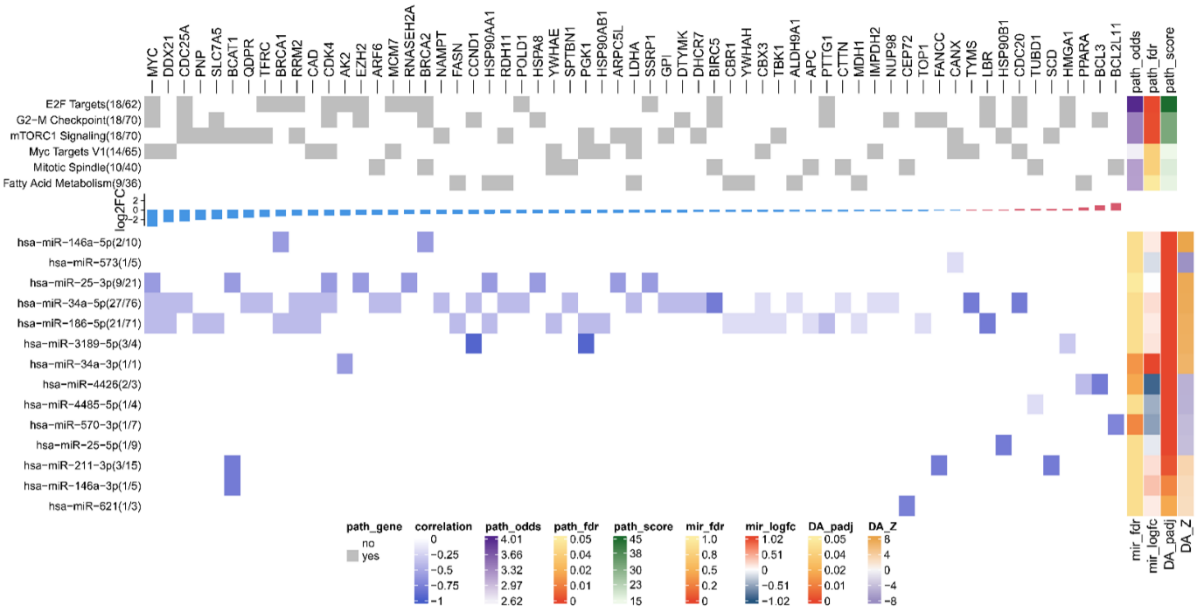

Figure 4: Pathway enrichment analysis results. The top heatmap shows the significantly enriched hallmark pathways and their associated genes that are targeted by the driver miRNAs. The middle bar plot shows the distribution of log2 fold-change of the genes (blue: downregulation, red: upregulation). The bottom heatmap shows the Spearman correlation coefficients between miRNAs and their target genes that are enriched in the hallmark pathways, with darker colors representing higher correlation values. The annotation bars represent the results of gene set enrichment analysis and differential gene expression and regulatory activity analysis. This includes pathways' odds ratio, adjusted p-value, and combined score and miRNAs' log2 fold-change and regulatory activity in Z-score normalization with the corresponding adjusted p-values.

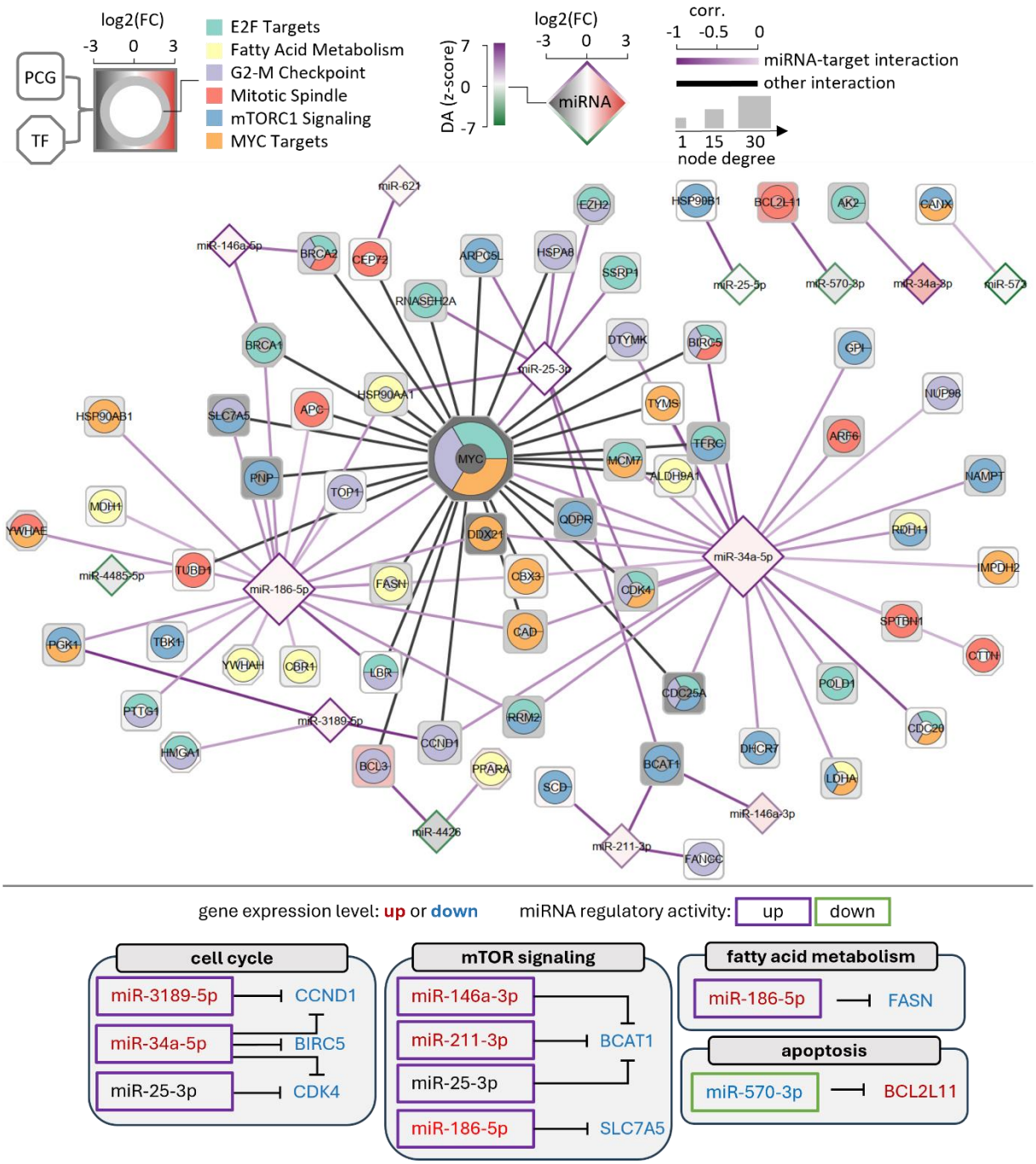

Figure 5 The identified key miRNA-gene interactions in the UM network. The shape of the nodes represents different molecular species, including protein-coding genes (PCGs; squares), TFs (octagons), and miRNAs (diamonds). The ring chart embedded in the PCG and TF nodes represents their associations with enriched hallmark terms. Node color represents the log2 fold-change of gene expression profiles. The edge color of the miRNAs represents changes in regulatory activities normalized using the z-score method. Node size increases with node degree. Line color represents different types of interactions, with miRNA-target interactions shown in a purple gradient quantified by correlation coefficients. Further details, including references, cell phenotypes and cancer types, of the identified microRNA-gene interactions can be found in SM Excel S6. The bottom figure summarizes the identified functional miRNA-gene interactions that are discussed in the main text. The font color indicates whether a gene is significantly up (red) or downregulated (blue). The window indicates whether a miRNA has a significant upregulation (purple) or downregulation (green) in regulatory activity.